

## (51) Full-scale testing of rock fall barriers for small-scale impact energy

### 小規模エネルギー吸収型落石防護柵の実規模実験について

ベルゲル クリストフ\*, 西田 陽一\*\*, 藤井 智弘\*\*\*

Christoph Berger, Yoichi Nishita, Tomohiro Fujii

\* 修(工), (株)プロテックエンジニアリング, 技術開発部 (〒957-0106 新潟県北蒲原郡聖籠町蓮潟 5322-26)

\*\* (株)プロテックエンジニアリング, 技術開発部 (〒957-0106 新潟県北蒲原郡聖籠町蓮潟 5322-26)

\*\*\*博(工), (株)プロテックエンジニアリング, 製造部長 (〒957-0106 新潟県北蒲原郡聖籠町蓮潟 5322-26)

*Rock fall barrier, Full-scale test, Impact force, Impact energy absorption*

防護柵, 実物実験, 落石, 衝撃, 吸収エネルギー,

### 1. Introduction

The present rock fall protection fence is a useful mitigation against small-scale rock fall hazard for which the distance between source and impact point is relatively short. For less accessible sites, or for a small environmental impact, this small-scale protection system can be installed without the need

of heavy equipment and materials.

In this report, two types of this protection fence are tested by varying span width and post height. The rock fall is simulated by a traditional pendulum set up at which the rock of 470kg is lifted up to 21.7m. The energy transformation at the energy dissipator devices are observed and analyzed closely.

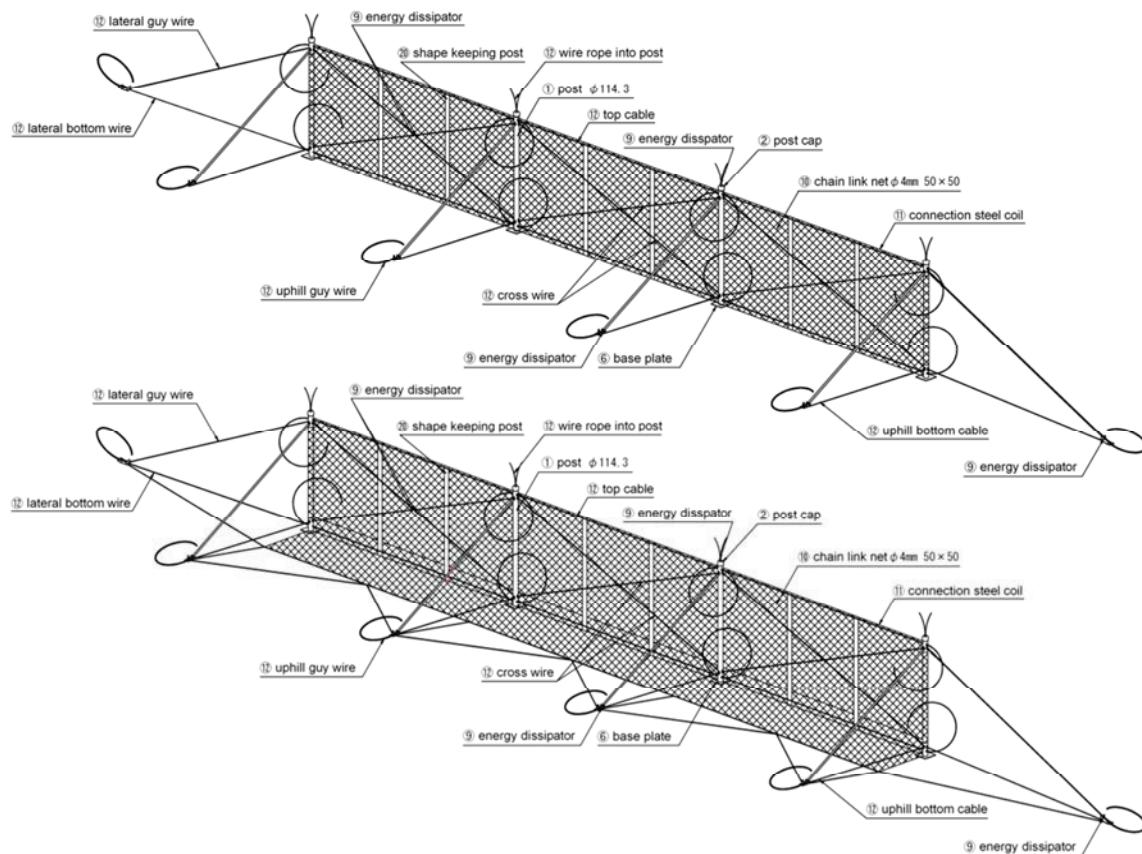


Figure 1: Arc Fence N-Type (up) and Arc Fence P-Type (down)

Table 2: test cases

Test No.	Arc Fence Type	Post [m]	Span [m]	Rock mass [kg]	Falling height [m]	Impact energy [kJ]	Loaded span	Impact position
N-02-01	N	2	5	470	21.7	100	middle	1/2 H
N-02-02	N	2	7	470	21.7	100	middle	1/2 H
N-02-03	N	2	10	470	21.7	100	middle	1/2 H
N-03-01	N	3	5	470	21.7	100	middle	1/2 H
N-03-02	N	3	7	470	21.7	100	middle	1/2 H
N-03-03	N	3	10	470	21.7	100	middle	1/2 H
N-03-04	N	3	10	470	21.7	100	middle	2/3 H
N-03-05	N	3	5	1007	13.2	130	side	2/3 H
P-02-01	P	2	5	470	21.7	100	middle	1/2 H
P-02-02	P	2	7	470	21.7	100	middle	1/2 H
P-02-03	P	2	10	470	21.7	100	middle	1/2 H
P-03-01	P	3	5	470	21.7	100	middle	1/2 H
P-03-02	P	3	10	470	21.7	100	middle	1/2 H

## 2. Test Outline and Test Purpose

The carried out test shall approve the structural safety of two different types of small-scale rock fall barriers. Namely, these are the ARC FENCE corresponding to 100kJ rock impact energy (hereafter N-Type) and the new developed POCKET STYLE ARC FENCE, of which an additional uphill extension of the wire net avoids the caught rock of rolling round the wire net (hereafter P-Type). Since the range of the experiment loads covers the design loads, the experiment results approve the structural safety of this rock fall protection system. The current report gives a summary of the test and its results.

### 2.1 Goals for the N-Type

- (1) Examining of the maximum global displacement of the fence by varying the span width.
- (2) Evaluating the behavior of the fence at a rock impact of 130kJ energy.

### 2.2 Goals for the P-Type

- (1) Confirmation of the structural safety for the whole set of 2m high posts and for the whole set of 3m high posts.
- (2) Examining of the maximum global displacement of the fence by varying the span width.
- (3) Checking the structural safety of the uphill anchor since this anchor is loaded by additional loads from the pocket wire ropes. Concerning the P-Type, the fences of 2m post height and 7m respectively 10m span width failed. Therefore these two last fences will not be used as protection structures.

## 3. Test Set up

### 3.1 Test Objects

Figure 1 shows the N-Type and the P-Type of the tested Arc

Table 1: arrangement of the friction devices

Part	Arrangement type		Number of friction device		Number of cables		Friction force [kN]	
	N-Type	P-Type	N-Type	P-Type	N-Type	P-Type	N-Type	P-Type
Lateral guy wire	F	F	2	2	2	2	20	20
Uphill guy Wire	F	F	2	2	2	2	20	20
Main top cable	F	F	1	1	2	2	10	10
Main bottom cable	F	F	1	1	2	1	10	5
Post heads	F	F	1	1	2	2	10	10
Cross wire	M	M	1	1	2	2	5	5

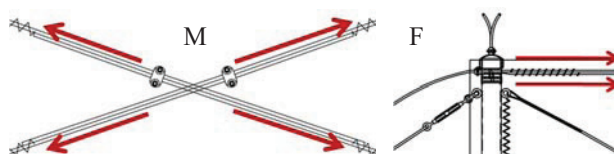


Figure 2: slipping direction at the friction devices

Fence. Three spans were assumed to be necessary for all tests. Table 1 shows the arrangement of the slipping cables at the friction devices. For a Type-F, both friction cables are slipping in the same direction at the device. Whereas the friction cables of a Type-M are slipping in opposite directions. Please, refer to Figure 2. The only difference between the friction devices of the N-Type and of the P-Type consists in the friction force at the bottom main cable. For the P-Type, it is only half strong as for the N-Type, as the uphill pocket gives additional stiffness.

### 3.2 Test Cases

Table 2 shows the experiment cases. Both, the span width and the post height are varying. The position of the impacting rock is for the 2m high cases at mid-height of the posts, whereas the position varies between 1/2 and 2/3 of the post height for the 3m posts. Moreover, the impact energy at the test exceeds up to 1.3 times the design energy.

### 3.3 Subjects of Measurement

- In the executed test, various measurements have been taken.
- (1) The acceleration of the rock in the three principal directions. (The maximum possible measurement is limited by the strain gauge regulations up to 100g.)
  - (2) The two optoelectronic sensors trigger the high speed camera and the release device of the rock. Additionally, they confirm the speed of the rock.
  - (3) The tension at the wire ropes is measured by strain gauges. (Avoiding the bending strains by two strain gauges applied in a half-bridge strain gauge circuit.)
  - (4) Shooting the impact with the high-speed camera from the side-view: confirming the rock speed just before impact,

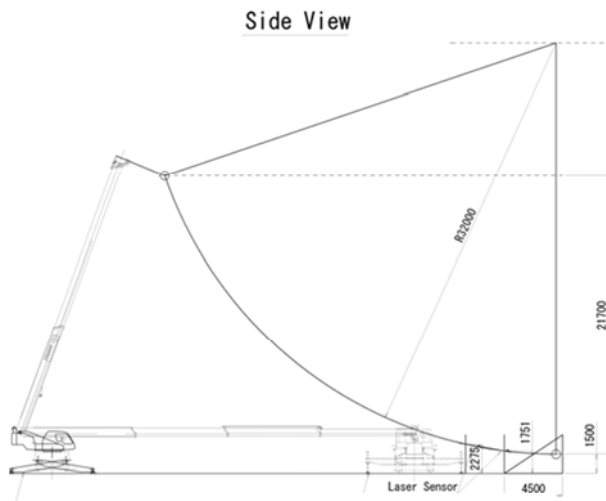


Figure 4: pendulum set up of the test

observing the propagating deformation and measuring the maximum displacement.

(5) Digital cameras at a lateral angle and in front of the fence: observing the propagating deformation.

(6) Measuring the length of the slips at the friction devices.

(7) Measuring the global displacement of the whole protection structure.

### 3.4 Test Procedure

(1) The Arc Fence is constructed accordingly on solid soil.

(2) The three-directional accelerometer is set in the center of the rock by assuring having the main direction of measurement (100g) parallel to the direction of the impact.

(3) Inserting a steel plate into the wires towards the uphill anchors as well as towards the side anchors. By use of a half-bridge strain gauge circuit, the tension is separated from bending effects.

(4) In order to shoot the propagating deformation of the fence, the high speed camera is placed. (500 pictures/second)

(5) The main crane (50t) lifts its top to the center of the arc of the prescribed rock's motion. The vertical line from the rock to the top is set to be just in front of the fence. The secondary crane (25t) pulls the rock up to the height of the corresponding impact energy. A proper arc must be ensured by the pulling from the secondary crane. The release at the secondary crane lets the rock swing. The release at the main crane is executed as the rock is in horizontal motion at the height of the defined impact location.

(6) The optoelectronic sensors are placed as displaced pairs in front of the fence. Although the displacement serves for speed measuring, the main task of the sensors is to trigger the release of the main crane and to trigger the measurements by the high speed camera and by the strain gauge measurements.

(7) The resulting strains as well as the high speed shooting are stored to the recording medium (HDD).

The loading situation of the test and the arc by the swing of the rock are shown in Figure 3 and in Figure 4.



Figure 3: test set up ready to release

Table 3: summary of the test results

Test No.	Maximum displacement [m]	Impact force [kN]	Impact energy [kJ]	Absorbed energy		Structural safety
				[kJ]	[%]	
N-02-01	3.5	-	100	57	57	OK
N-02-02	4.5	59	100	71.7	71.7	OK
N-02-03	4.8	39	100	77.1	77.1	OK
N-03-01	3.5	59	100	61.3	61.3	OK
N-03-02	4.2	61	100	83.3	83.3	OK
N-03-03	4.7	44	100	68	68	OK
N-03-04	4.8	51	100	-	-	OK
N-03-05	3.5	89	130	61.7	47.5	OK
P-02-01	2.7	79	100	57.4	57.4	OK
P-02-02	3.5	76	100	28.7	28.7	NG
P-02-03	-	29	100	39.1	39.1	NG
P-03-01	3.7	60	100	68.3	68.3	OK
P-03-02	3.8	81	100	58.7	58.7	OK

## 4. Test Results

### 4.1 Summary of the Results

For the N-Type, all fences have completely absorbed the falling rock loaded by an impact energy of 100kJ. The fence, which was facing an impact energy of 130kJ, has stopped the falling rock as well, although the posts were damaged. Based on the results, following can be said:

(1) Fences by post heights of 2m and 3m and by a span varying from 5m to 10m are all able to catch and stop the impacting rock of a 100kJ energy load.

(2) There is no problem about the position of the falling rock into the fence, because even at a worst case scenario of 2/3H on the posts (case N-03-04 and N-03-05), the rock could be caught and stopped. In other words, for a post height of 2m, the performing height of 1m of the fence is approved respectively a performing height of 2m for a fence of 3m high posts.

(3) In experiment N-03-05 with the severest conditions, it seems that the design energy of 100kJ can be exceeded by a factor of 1.3. Though, some damaged components must be

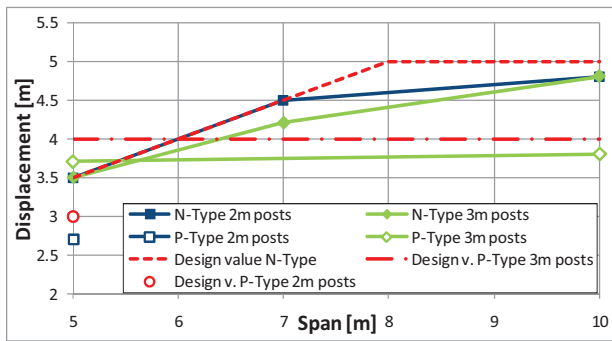


Figure 5: displacement of the fence at impact

replaced (see right-side middle picture in Figure 6).

Concerning the test of the P-Type, the impacting rock could be caught and stopped for a span of 5m for the 2m high fences and for spans of 5m and 10m at the 3m high fences. Based on the results, following can be said:

- (1) The maximum allowable span for a 2m high fence does not exceed a width of 5m.
- (2) At fences of a height of 3m, all possible spans from 5m to 10m can be allowed.

#### 4.2 Deformation

Figure 5 shows the relation of the maximum displacement by the span width. This result is obtained by the pictures of the high speed camera (Figure 6). For the N-Type, following can be said:

- (1) The narrower the span width is, the smaller the maximum displacement becomes.
- (2) There is no significant difference in the maximum displacement of a 2m or a 3m post height.
- (3) The design value of the maximum displacement can be set as the red regularly dashed line in Figure 5 is indicating.

Following different conclusions are made for the P-Type:

- (1) There is only a negligible influence of the span width on the maximum displacement for fences of 3m posts.
- (2) Comparing at a span width of 5m, the maximum displacement for the fence of 3m posts is about 1m bigger than for the fence of 2m posts.
- (3) As in Figure 5 indicating, the design value of the maximum displacement can be set as the red irregularly dashed line for the fence of 3m posts and as the red circle for the fence of 2m posts.

#### 4.3 Energy Absorption Devices

After the impact, the slip of each cable at the corresponding friction device has been measured. These measurements and the in Table 1 defined friction forces, which are assumed as constant, give the absorbed energy. The results are in Table 3.

- (1) The horizontal main cable (top and bottom) friction devices as well as those of the cross wire contribute most to the absorbed energy. The slip at the post heads, at the lateral and at the uphill guy wires is insignificant and quasi zero.

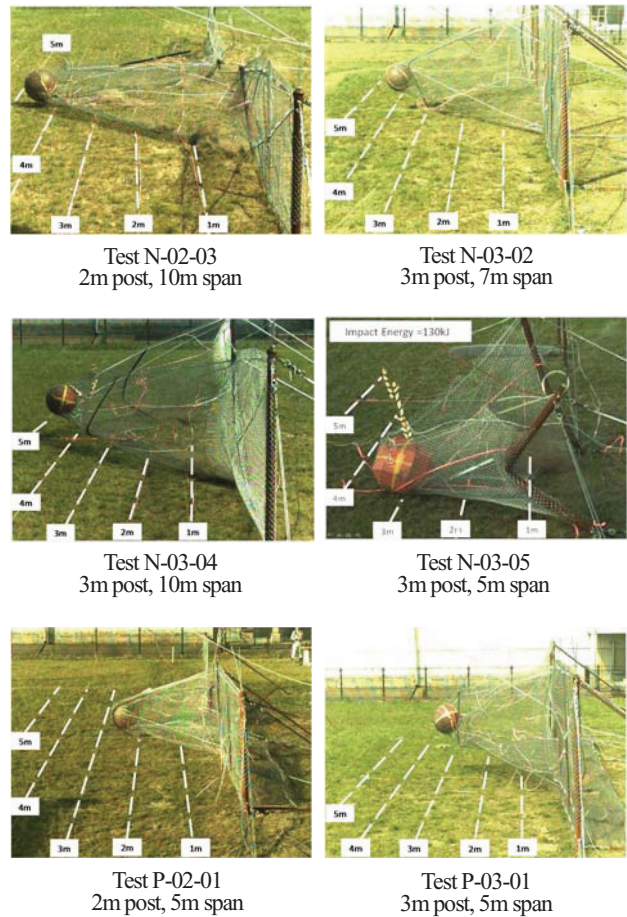


Figure 6: max. displacement by the high speed camera

- (2) For all cases except case N-03-05 (impact energy 130kJ), the ratio of the absorbed energy by the impact energy varies between 60% and 80% for the N-Type and between 60% and 70% for the P-Type.

- (3) In Test N-03-05 (impact energy 130kJ), the absorbed energy - impact energy - ratio is only about 50%. This low value seems to base on the fact, that the impact was into an end-span, which is more constrained in its general displacement than a middle-span. Moreover, the end post was strongly bent during the impact.

#### 4.4 Impact Force

- (1) As for the N-Type, the impact force tends to decrease by increasing the span width (Figure 10). The wider spans give more room for an extension of the wire net, which seems to have a positive influence on the impact force.

- 2) Contrary to the N-Type, the impact force for the P-Type increases by increasing the span width. To understand such behavior, it is important to know, that the pocket is always constructed the same way regardless of the span width. The constraining influence of the fixed pocket becomes important for wide spans. The deformation of the pocket indicates this, too.

- (3) The impact force at the fence is about a 1/10 of the impact force of a rock into a sand cushion layer (see Equation 1). This

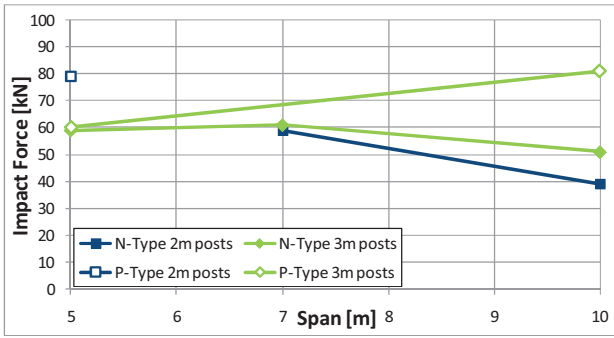


Figure 10: max. impact forces based on measured decelerations

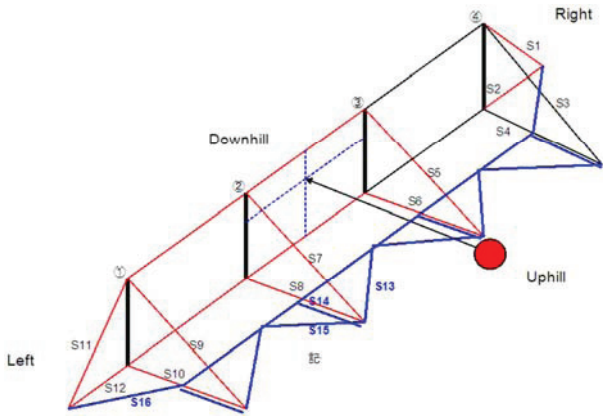


Figure 8: location of each wire rope

soft catching by the protection structure enables it to resist against such heavy impact loads.

$$P_{\max} = 2.108 (m \cdot g)^{2/3} \cdot \lambda^{2/5} \cdot H^{3/5} = 5864 \text{ kN} \quad (1)$$

P: impact force on a sand cushion layer  
 m: rock mass 0.47 t  
 g: gravity 9.81 ms<sup>-2</sup>  
 λ: Lamé coefficient 1'000 kNm<sup>-2</sup>  
 H: falling height 21.7 m

#### 4.5 Wire Tension

Table 4 shows the maximum tension at each wire rope, which is generated during the rock impact tests. The location of each wire rope is indicated in Figure 8, at which the wire ropes of the pocket (blue) do not exist for the N-Type. One wire rope tension in function of time as a representative is chosen for both the N-Type and the P-Type. Therefore, the tension in the guy wire of post 2 at test N-03-02 and at test P-03-01 is presented in Figure 7 respectively in Figure 9. The following is observed for the N-Type, which is less stiff than the P-Type:

- (1) The maximum tension which arises in a lateral guy wire rope is 26.7kN during the test N-03-04. The maximum tension for an uphill guy wire was 27.4kN at test N-03-05.
- (2) The average tension (blue line in Figure 7) of the time depending tension of post 2's uphill guy wire (red line) begins at a local maximum of the early stage (0.18s) and ends at its major attenuation (0.38s). On one hand the average tension of about 18kN stays below the friction force of the energy dissipator of

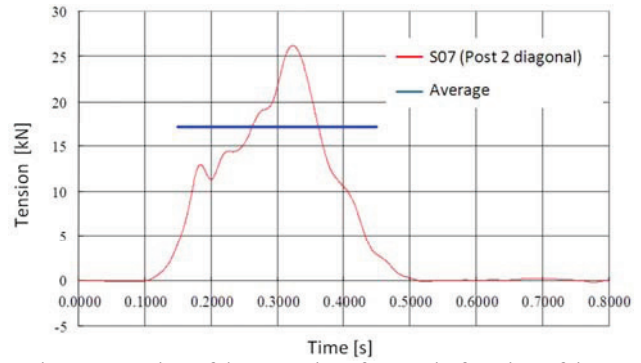


Figure 7: tension of the guy wire of post 2 in function of time N-03-02

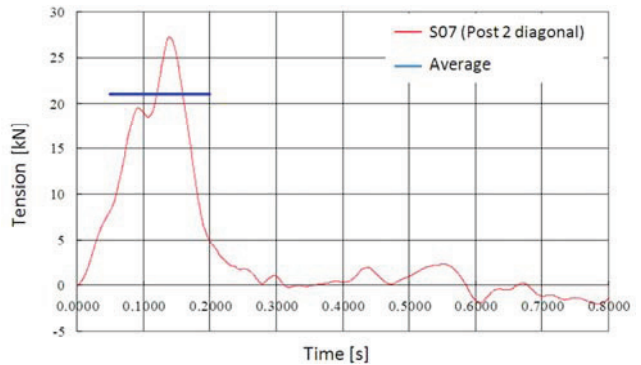


Figure 9: tension of the guy wire of post 2 in function of time P-03-01

20kN and on the other hand, the actual measured tension force of 26.3kN exceeds clearly this friction force. But anyhow, no slipping could be measured at the energy dissipator after the test because there was no slipping.

(3) Concerning the previous point, the effective anchor resistance is significantly higher than its design value of 20kN, as the effective force of 27.4kN did not cause any damage at the anchor.

(4) Concerning the maximum effective shearing force at the lateral anchor, a conservative calculation by an addition of the maximum measured tension out of the two lateral guy wires and of the maximum measured tension out of the two lateral bottom wire ropes is chosen. This gives us the shearing force  $S_{\max}$  of 40.6kN (= maximum lateral guy wire tension of 26.7kN x cosines of the actual appearing angle towards the horizontal of 33.7° + maximum lateral bottom wire tension of 18.4kN). It is clearly below the anchor-bolt's characteristic shear resistance (Equation 2). Therefore, the structural safety of the lateral anchor can be satisfied in regards to shearing.

$$S_y = A_s \cdot \left( \frac{\sigma_y}{\sqrt{3}} \right) = 435 \times \frac{450}{\sqrt{3}} \times 10^{-3} = 113 \text{ kN} \quad (2)$$

$S_y$ : characteristic anchor-bolt's shear resistance  
 $A_s$ : cross sectional area of the anchor bolt 435mm<sup>2</sup>  
 $\sigma_y$ : yield stress 450MPa

(5) The same calculation has been done for the uphill anchor. The resulting shear force  $S_{\max}$  is 38.3kN

Table 4: wire rope tension of each location [kN]

Test No.	left end diagonal	left end bottom	right end diagonal	right end bottom	Post 1 diagonal	Post 1 bottom	Post 2 diagonal	Post 2 bottom	Post 3 diagonal	Post 3 bottom	Post 4 diagonal	Post 4 bottom	Pocket Post 2 right	Pocket Post 2 middle	Pocket Post 2 left	Pocket left end diagonal
Test No.	S11	S12	S1	S2	S9	S10	S7	S8	S5	S6	S3	S4	S13	S14	S15	S16
N-02-02	14.4	3.4	11.4	0.9	4.4	0.3	21.0	2.5	14.6	5.3	0.4	5.5	X	X	X	X
N-02-03	14.7	3.1	15.0	0.8	0.2	0.3	13.3	4.0	20.6	15.5	0.1	0.0	X	X	X	X
N-03-01	15.2	0.7	13.1	0.9	3.0	0.9	17.2	2.2	17.8	2.2	1.3	0.4	X	X	X	X
N-03-02	18.6	2.4	22.0	0.2	1.0	0.5	26.3	3.3	23.9	0.4	0.5	0.4	X	X	X	X
N-03-03	23.6	8.2	24.0	2.5	8.7	1.0	21.4	0.3	17.9	6.5	3.3	1.4	X	X	X	X
N-03-04	25.9	2.4	26.7	1.1	3.8	0.2	X	10.1	19.9	5.8	2.3	0.5	X	X	X	X
N-03-05	X	18.4	16.3	0.9	27.4	15.5	25.4	14.9	0.3	0.3	0.0	0.8	X	X	X	X
P-02-01	16.4	1.4	20.2	0.1	1.6	4.9	24.2	1.0	25.2	5.7	0.6	0.0	15.6	X	1.3	10.6
P-02-02	17.6	2.7	21.6	0.5	20.6	3.3	0.2	1.3	30.1	0.0	1.1	0.1	9.1	6.1	0.2	14.7
P-02-03	10.8	2.4	17.4	0.4	0.1	0.7	0.1	13.4	12.7	0.4	0.1	0.2	8.4	3.3	0.1	13.5
P-03-01	6.4	2.9	11.5	0.0	0.0	4.1	27.2	1.7	20.0	1.3	1.0	0.5	4.3	2.6	0.0	9.8
P-03-02	17.8	1.1	15.1	0.5	0.8	0.9	X	3.4	13.0	12.4	1.0	1.3	17.0	5.5	0.1	19.9

Again, structural safety, in regards to shearing of the anchor bolt, is given.

The following points can be concluded on the results of the P-Type, of which the pocket creates an additional fixation:

(1) Disregarding the tests P-02-02 and P-02-03 of failed structures, the maximum tension in a lateral guy wire occurs at 20.2kN for test P-02-01, whereas the maximum tension of a uphill guy wire arises to 27.2kN at test P-03-01.

(2) The average tension (Figure 9) of the time depending tension of post 2's guy wire (red line) begins at a local maximum of the early stage (0.09s) and ends at its major attenuation (0.16s). The friction force of the energy dissipator of 20kN is clearly passed by the maximum measured tension of 27.2kN and slightly exceeded by the average tension of 21kN. This time, a slip of 10mm could be measured at the corresponding friction device.

(3) Since the friction force of 20kN is only exceeded for a short duration of about 0.05s, and since this observation of a slip could only be done at such a detailed experiment, this friction force will not be a problem for a real case design, as there won't be excessive deformations due to slip at the guy wires.

(4) Concerning the previous two points, the effective anchor resistance is significantly higher than its design value of 20kN.

(5) Besides an additional bottom cable of the pocket side, the shear resistance calculations of the anchor-bolt for the P-Type are done in a similar way as for the N-Type.

The effective shearing force at the lateral anchor is calculated as a value of 39.6kN. ( $= \cos 33.7^\circ \times 20.2\text{kN} + 2.9\text{kN} + 19.9\text{kN}$ ).

The structural safety of shear at the anchor-bolt is approved.

(6) The shearing of an uphill anchor-bolt is approved as well.

The characteristic shear resistance of 113kN is clearly not exceeded by an effective force of 58.8kN ( $= \cos 33.7^\circ \times 27.2\text{kN} + 12.4\text{kN} + 17.0\text{kN} + 5.5\text{kN} + 1.3\text{kN}$ ).

## 5. Conclusion

Primarily, the executed series of tests on the N-Type as well as on the P-Type approve the structural safety for these structures. Nevertheless, a clear answer to the resulting maximum displacement was created as well. Hence, a difference in the stiffness of the N-Type and P-Type is considered. Generally, the soft and ductile catching results of the Arc Fence could be seen in the deformations, the forces and in the slips at the energy dissipators.

## References

- 1) Japan Highway Association, *Rock Fall Measurement Manual*, (2000) Tokyo, Japan. (in Japanese)
- 2) Japan Society of Civil Engineering, Structural Engineering Committee Impact Issue Research Subcommittee (1995), *Practical Methods for Impact Test and Analysis*, (2004) Tokyo, Japan (in Japanese)